Original Article

TIPS Trends in Pharmaceutical Sciences 2022: 8(3): 155-164.

Taguchi design optimization of curcumin loading in mesoporous silica nanoparticles with variable particle and pore sizes

Mina Shafiee[1], Samira Sadat Abolmaali[1,2*], Mozhgan Abedanzadeh[2,3], Ali Mohammad Tamaddon[1,2]

[1]Center for Nanotechnology in Drug Delivery, Shiraz University of Medical Sciences, Shiraz, Iran.
[2]Pharmaceutical Nanotechnology Department, Shiraz School of Pharmacy, Shiraz University of Medical Sciences, Shiraz, Iran.
[3]Student Research Committee, Shiraz University of Medical Sciences, Shiraz, Iran.

Abstract

Mesoporous silica nanoparticles (MSNs) have received a lot of attention due to their wide range of applications in the delivery of poorly soluble phytochemicals like curcumin (CUR). Given that pore diameter and particle size determine the specific surface area, as well as drug loading in mesoporous nanoparticles, in the present study, we developed MSNs with varying pore sizes to investigate their effects on CUR loading. Dynamic light scattering (DLS), field-emission- scanning electron microscopy (FE-SEM), and Brunauer-Emmett-Teller (BET) analyses were used to characterize the MSNs. CUR was loaded into MSNs using solvent evaporation method, and the drug loading was determined using UV spectroscopy. Results revealed that the MSN synthesis condition had a significant effect on pore size and particle diameter. According to FE-SEM micrographs, MSNs had a nearly spherical shape. DLS results indicated particle sizes ranging from 25 to 100 nm. According to the BET findings, pore size and specific surface area varied in range of 4 - 8 nm and of 570 - 1180 m2/g, respectively. In addition, CUR loading efficiency and loaded amount were 75% and 33% in optimal conditions, respectively. These findings supported the use of MSNs to load and deliver CUR as a poorly soluble drug in a variety of pathophysiological conditions.

Keywords: Mesoporous silica nanoparticles, Pore size, Particle size, Surface area, Drug loading, Curcumin.

Please cite this article as: Mina Shafiee, Samira Sadat Abolmaali, Mozhgan Abedanzadeh, Ali Mohammad Tamaddon. Taguchi design optimization of curcumin loading in mesoporous silica nanoparticles with variable particle and pore sizes. Trends in Pharmaceutical Sciences. 2022;8(3):155-164. doi: 10.30476/TIPS.2022.95646.1150

1. Introduction

Curcumin (CUR), a hydrophobic natural polyphenol derived from Curcuma longa, exhibits a wide range of pharmacological properties, including antioxidant, anti-inflammatory, and antimicrobial properties. However, its medical applications have been hampered by its low solubility and bioavailability. CUR has an extremely low solubility at pH values ranging from 1.2 to 7.4, which are physiological pH values of the gastrointestinal tract. Moreover, CUR is prone to rapid autooxidation and hydrolysis in alkaline aqueous solutions, undergoes photodegradation, and has a short half-life due to rapid pre-systemic metabolism in the intestinal wall (1). Numerous delivery systems have been suggested to address these issues, including CUR microencapsulation in liposomes (2), polymeric micelles (3, 4), conjugates (5), and inorganic nanoparticles such as mesoporous silica nanoparticles (MSNs).

Over the last decade, a plethora of inorganic nanoparticles have been produced for drug de-

Corresponding Author: Samira Sadat Abolmaali, Department of Pharmaceutical Nanotechnology, School of Pharmacy, Shiraz University of Medical Sciences, Shiraz, Iran
Email: s.abolmaali@gmail.com

Received: 12/03/2022; Accepted: 01/09/2022

livery. MSNs have several advantages, including a unique structure with tunable pore and particle sizes, a high specific surface area, ease of functionalization, and high biocompatibility. Silica materials are classified as "Generally Recognized as Safe" (GRAS) by the FDA and are used in cosmetics and as a food-additive. Their porous structure allows for a high drug loading as well as modified drug release (6-8). Advancements in the synthesis of MSNs with controlled particle size, morphology, and porosity, as well as their chemical stability, have made silica matrices appealing in drug delivery (8-10). MSN delivery systems have shown to improve CUR solubility and bioavailability (1, 11-13), pH-sensitive release (14, 15), redox-sensitive release (16), targeted delivery (10, 17-19), and combined bioimaging (20). According to the literature, nearly 12% CUR can be dissolved after 25 h in phosphate buffer (pH 7.4, 37 °C), indicating that free CUR has a sustained dissolution profile (17). However, depending on the MSN physical characteristics and surface chemistry, MSN loading has shown enhanced CUR dissolution/release (16, 17).

MSN synthesis follows a self-assembly mechanism in which reactant ratios and experimental conditions control the physical, chemical, and structural properties of the nanoparticles. Cationic cetyltrimethylammonium bromide (CTAB) surfactant is commonly employed in the synthesis of MSNs as a porogen due to strong electrostatic interactions with silica precursors, resulting in MSN pore sizes of about 3 nm. For successful drug delivery applications, MSNs with larger mesopores and homogenous particle size distribution are often required (8). To this aim, we designed MSNs with tunable pore and particle sizes for high-capacity loading of poorly soluble drugs (21). The synthesis approach entails the hydrolytic condensation of a tetraorthosilicate (TEOS) precursor and the polymerization of methyl methacrylate (MMA) at the same time in a homogeneous dispersion of n-heptane in water. We previously demonstrated that pore sizes could be tailored in range of 2-7 nm while maintaining a high specific surface area (600-1200 m^2/g). Moreover, different volume ratios of n-heptane/water produced sizes ranging from 25 to 100 nm (22). In another study, mesoporous silica nanocomposites made of polymerized alkyl methacrylate monomers such as methyl methacrylate, butyl methacrylate, or a mixture of methyl methacrylate and acrylic acid have been used to improve silibinin dissolution and antioxidant activity. Nanoparticles had a spherical shape, a small size (20 nm), a substantial pore volume (1.6 cm3/g), and a significant silibinin loading (19%) (23). In the present study, we utilized Brunauer-Emmett-Teller (BET), field emission - scanning electron microscopy (FE-SEM), dynamic light scattering (DLS), and UV spectroscopy methods to investigate the effect of MSN surface area on CUR loading parameters.

2. Materials and methods

2.1. Materials

Tetraethyl orthosilicate (TEOS) was supplied from Merck (Germany). Cetyltrimethylammonium ammonium bromide (CTAB) was purchased from DaeJUNG (South Korea), while methyl methacrylate (MMA), L-lysine, and 4,4′-Azobis (4-cyanovaleric acid) (ACVA) were supplied from Sigma-Aldrich. All aqueous preparations were made from deionized water prepared by MilliQ3 (Millipore, USA).

2.2. MSN preparation

In a typical reaction, 300 mg CTAB was dissolved in 96 mL of deionized water. At 70 °C, the mixture was N2-purged for 45 min. Variable amounts of n-heptane (6, 27 and 45 ml) were then added to the CTAB solution. 0.5, 9 and 20 mg/ml of MMA, 66 mg L-lysine, 3000 mg TEOS, and 0.81 mg/ml ACVA were added to the reaction vessel after 15 min. After 4 h, the reaction was cooled down to room temperature, and the organic phase was decanted before removing the organic template by calcination at 500 °C for 5 h.

2.3. MSN characterization

Specific surface area (SSA) and pore size of each sample were determined using nitrogen adsorption/desorption isotherms (MicroActive for TriStar II Plus 2.03, Micromeritics, USA). FE-SEM (MIRA3, TESCAN, USA) was used to characterize the morphology of gold-coated samples. An in-situ particle size analyzer (NANO-Flex II,

Microtrac, Germany) was used to determine the particle size distribution and polydispersity of aqueous dispersions in 0.1 M phosphate buffer (pH = 7.4). ZETA-check (Microtrac, Germany) was also used to measure zeta potentials.

2.4. CUR loading

The MSNs were loaded with CUR using the solvent evaporation technique (24). A 5 mg/ml CUR solution in absolute ethanol was added to microtubes containing varying amounts of MSNs dispersed in absolute ethanol to achieve different drug/MSN ratios (0.1, 0.3, and 1 w/w), and the mixture was stirred overnight as described in the literature (16, 19, 25, 26). Samples were incubated in a shaking block (300 rpm) at different temperatures (5, 30, and 55 °C). N2 gas purging was used to remove the solvent, and the particles were re-dispersed in an ethanol-water (1:9 v/v) mixture for dissolving unloaded CUR, as similarly reported elsewhere (17). The loaded particles were then centrifuged for 30 min at 12,000 rpm to remove the unloaded CUR. The loaded amount of CUR was determined directly after solubilizing the loaded MSNs with 0.1 mL hydrofluoric acid, which was then diluted to 1 mL with absolute ethanol and detected using UV-visible spectroscopy at the CUR maximum wavelength (λ_{max} =427 nm). CUR concentration was calculated from the standard curve plotted for a series of standard solutions prepared in the concentration range of 3-100 µg/ml. Afterwards, the loading efficiency (LE%) (Eq. 1) and the loaded amount (LA%) (Eq. 2) were calculated using the following equations:

$$loading\ efficiency(\%) = \frac{W\ drug\ loaded}{W\ drug\ added} \times 100 \quad \text{(Eq. 1)}$$

$$loaded\ amount(\%) = \frac{W\ drug\ loaded}{W\ MSN\ added + W\ drug\ loaded} \times 100 \quad \text{(Eq. 2)}$$

2.5. Statistical design and analysis

Factorial experimental design techniques, such as Taguchi orthogonal array design, provide an efficient method for investigating the effect of multiple factors at the same time with a small number of experimental trials (27). L-9 Taguchi orthogonal array was designed for two composition variables (MSN sample type with varied SSAs and drug/MSN weight ratios) and two process variables (incubation time and temperature) in three levels (Table 1). Each experimental condition was repeated three times. Design Expert software (Ver. 8.0., Stat-Ease, Inc.) was employed for data analysis. A two-factor interaction (2FI) model and the Forward algorithm were used to incorporate significant terms identified by the ANOVA method into model equations. P values lower than 0.05 were considered statistically significant. Finally, the best condition for maximum desirability function (LE%×LA%) was chosen and validated using triplicate confirmatory testing.

3. Results and discussion

3.1. Physicochemical properties of MSNs

MSN synthesis were accomplished by sol-gel of a silica precursor (TEOS) using CTAB as a soft template and L-lysine as a base catalyst (28). The conventional Stöber sol-gel method was modified in this study to include ACVA-initiated free radical polymerization of methyl methacrylate for preparing hybrid organic-inorganic nanocomposites, which were then calcined to produce MSNs with varying particle and pore sizes (21). FE-SEM, XRD, BET, and DLS techniques were used to characterize the morphology, pore size, and particle size of MSNs. The FE-SEM micrograph (Figure 1) showed small spherical aggregates. The pore characteristics of the MSNs were determined using N2 adsorption/desorption isotherms. Table 1 summarizes the BET results. Pore diameters varied from 4.8 to 7.2 nm. In addition, SSA decreased from 1180 to 570 m2/g by increasing n-heptane volume. When compared to MSNs reported for CUR loading (10, 19, 25, 26, 29-33)

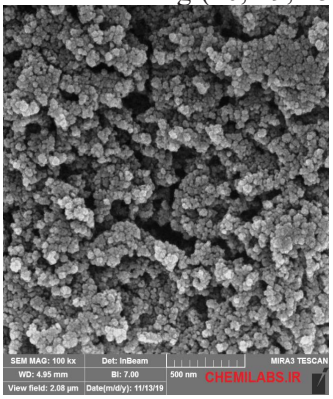

Figure 1. FE-SEM micrograph of MSNs (P3).

Table 1. Hydrodynamic diameter, pore size, and specific surface area (SSA) of MSN samples.

MSN sample	n-hexane volume (ml)	MMA concentration (mg/ml)	Mean hydrodynamic diameter (nm)	Pore size (nm)	Surface area (m2/g)	Zeta potential (mV)
P0	0	0	100	4.8	1180	-9.1
P1	6	0.5	45	5.5	743	-8.3
P2	27	9	40	5.0	570	-8.6
P3	45	20	25	7.2	612	-8.5

with pore sizes in the range of 2.5-7.6 nm and SSA of 30-992 g/cm2, the MSNs prepared in the current study encompass large pore sizes and high SSA. The DLS results (Figure 2) revealed that increasing the n-heptane volume reduced particle sizes from 100 to 25 nm, as explained in the literature (22), because the n-heptane/water interface can adsorb nucleated particles and prevent their growth. Although decreasing particle size should increase SSA, increased pore sizes with a lower surface-to-volume ratio surpassed the particle size effect (22), resulting in the formation of particles with lower SSA (Table 1). The synthesized MSNs were relatively smaller compared to MSNs used for CUR loading with hydrodynamic diameters in the range of 64-197 nm, depending on the MSN fabrication process and reaction conditions (10, 26, 30, 32-37).

3.2. CUR loading in MSNs

CUR, a poorly water-soluble phytochemical drug, was loaded into the MSN nanocontainer. The solvent evaporation method, which is commonly used for MSN loading, was employed for CUR loading in temperatures ranging from 5 °C to 55 °C using ethanol as the solvent. Similarly, MSNs have been loaded with CUR in ethanol for 24 h at ambient temperature (10, 19, 25, 26, 38) or 37-40 °C (37, 39), ethanol-water (34), acetone (33), ethanol-acetone (30, 39), DMSO (32, 35), and dichloromethane (31), and the drug loading was determined using UV-visible spectroscopy. When CUR degradation in ethanol was compared to CUR degradation in water, the %decay/day was remarkably reduced from 1.17 to 0.05 (about 23 folds) at 30 °C, and ethanol was presented as the selected solvent with the highest compatibility among organic solvents (40). Higher incubation temperatures of 50-60 °C for CUR loading in ethanol were also reported in the literature (3, 4). Our preliminary analysis confirmed that the CUR UV-visible and fluorescence spectra (data not shown) remained unchanged after incubating the ethanolic solution of CUR at different temperatures (5, 30, and 55 °C), indicating that the solvent, time, and temperature conditions were applicable in CUR loading in MSNs. Although P0 (without n-hexane addition) had the highest SSA (Table 1), it did not result in an acceptable CUR loading (around 1% w/w in the highest drug/MSN ratio =1), possibly due to its small pore size, and was excluded from further analysis. In contrast, high LA% (41.4±2.6) and LE% (68.5±4.8) were obtained for P3 and P1, respectively, indicating a MSN type-specific CUR loading (23). Other studies have found that CUR loading in MSNs ranges from LA% =1.1 to 14.7% (17, 32, 36, 39). LA% as high as 45-50% have been reported in amine-functionalized MSNs (26) or large pores of guanidine-functionalized MSNs (33), emphasizing the importance of pore size and functionality in CUR loading. The synthesized MSNs in the present study had high LA% without any surface modification. Although CUR surface adsorption in MSNs can happen through inter-

Table 2. Independent factors influencing CUR loading in the MSNs and their levels.

Factor	Description	Low level	Medium level	High level
A	MSN sample (SSA, m2/g)	570	612	743
B	Time (h)	0.5	3	18
C	Curcumin/MSN weight ratio	0.1	0.5	1
D	Temperature (°C)	5	30	55

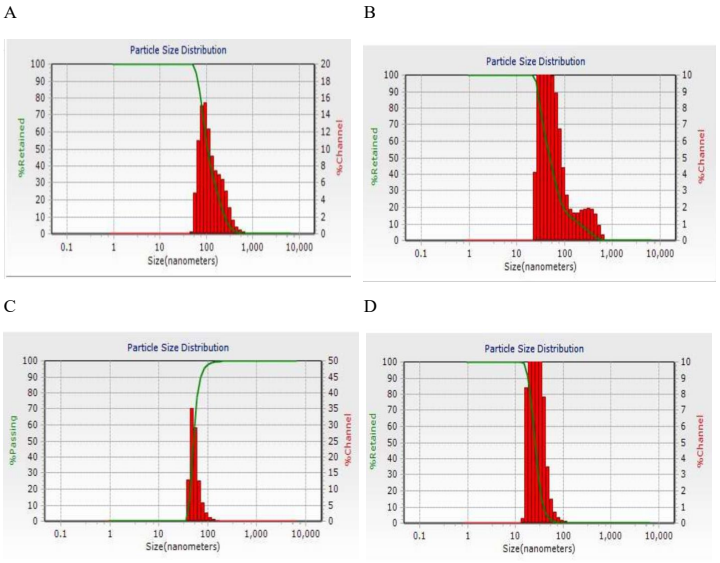

Figure 2. DLS histograms (intensity) for P0 (A), P1 (B), P2 (C), and P3 (D) samples in distilled water.

molecular interactions media (e.g., hydrophobic, hydrogen bonding, etc.), protonated CUR (pKa values of 7.8, 8.5, and 9.0) and deprotonated surface silanol groups may interact electrostatically in aqueous-organic mixtures. FTIR spectroscopy and adsorption isotherms are recommended for analyzing the drug loading mechanism in MSNs (41-43).

Table 2 summarizes factors and their respective levels considered when evaluating CUR loading parameters using the Taguchi design. According to ANOVA tables (see Supplementary File for details), the chosen 2FI models fit the experimental data satisfactorily ($P<0.0001$ for both LE% and LA% responses), and the block designation did not cause any interference. The Forward algorithm with adequate predictability ($r^2=0.98$ and 0.99 for LE% and LA%, respectively) was used to determine the significant model terms. As shown in Figure 3, after a short incubation time (0.5 h)

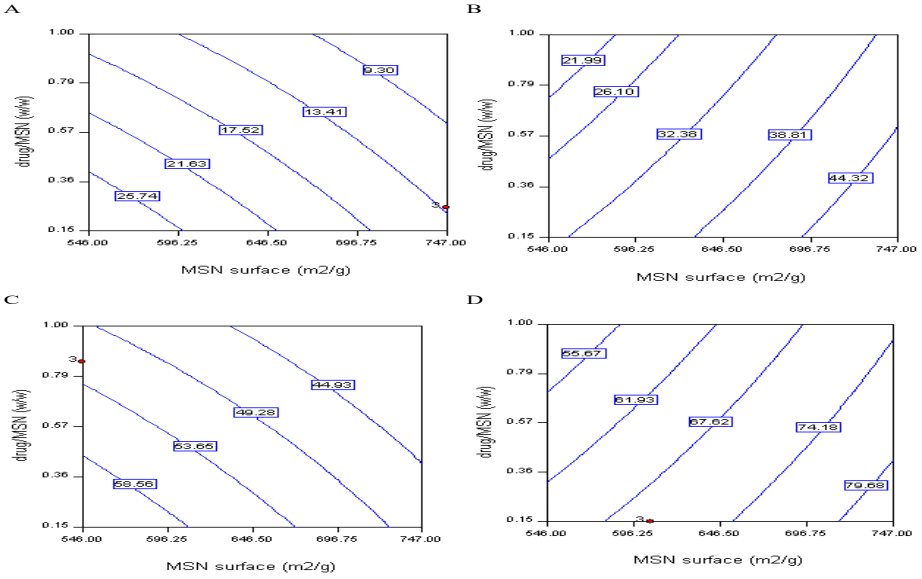

Figure 3. Curcumin loading efficiency (LE%) in different MSNs and drug (CUR)/MSN ratios, A: short time (0.5 h) and low temperature (5 °C), B: long time (18 h) and low temperature (5 °C), C: short time (0.5 h) and high temperature (55 °C), D: long time (18 h) and high temperature (55 °C).

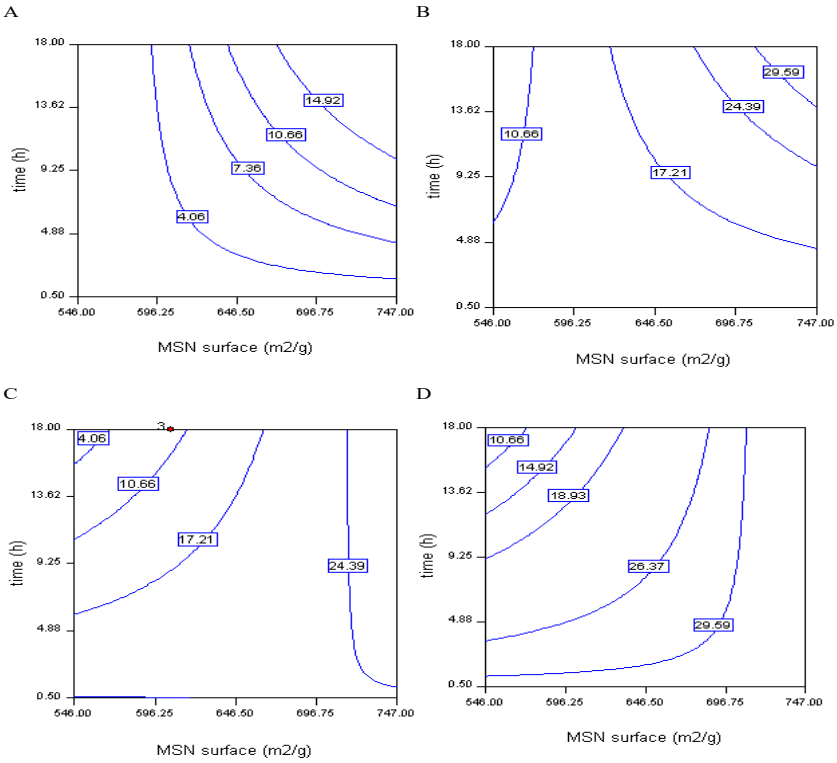

Figure 4. Curcumin loaded amount (LA%) in different MSN samples, A: low curcumin/MSN ratio (0.1) and low temperature (5 °C), B: high curcumin/MSN ratio (1) and low temperature (5 °C), C: low curcumin/MSN ratio (0.1) and high temperature (55 °C), D: high curcumin/MSN ratio (1) and high temperature (55 °C).

at 5 °C, the MSN sample with the highest SSA (P1) had a low LE%, which increased drastically when the temperature was raised to 55 °C. Furthermore, the MSN sample with a relatively low SSA and the largest pore size (P3) showed the highest LE% after 0.5 h. After a long incubation time (18 h), high LE% values were achieved even at low temperature (5 °C). Importantly, by increasing the CUR to MSN weight ratio, LE% was decreased. It appears that the loaded CUR can prevent further loading within mesopores and can progressively reduce SSA, resulting in a saturable adsorption pattern; thus, a lower proportion of added drug can be adsorbed within mesopores at higher dug concentrations. Abdous et al. also found that the LE% increases with incubation time and decreases with the CUR/MSN ratio. After a long incubation (18 h) at high incubation temperature (55 °C), the effect of CUR to MSN weight ratio on LE% became marginal. It seems that after a prolonged incubation time and a high temperature, drug diffusion into the mesopores and consequently LE% are enhanced regardless of the CUR to MSN weight ratio. Figure 4 shows that LA% increased as the CUR/MSN weight ratio increased. Moreover, LA% increased with increasing SSA as determined for P1. Regardless of incubation temperature, the effect of SSA was obvious after a long incubation time (18 h). The optimum condition was defined as P1 sample loaded with CUR (0.5 w/w) for 18 h at 55 °C, resulting in LA= 33% and LE= 75% with the prediction accuracy of 89.1% and 86.2%, respectively. Kuang et al. reported LA=8.1% and LE=89.1% for CUR loading on PEGylated MSNs (32). Mashayekhi et al. also found that the LE% for CUR-loaded MSNs was around 12.5% (44). Overall, the MSNs synthesized in this study surpass those reported in the literature for CUR loading under optimized conditions.

4. Conclusion

MSNs with variable particle sizes, pore diameters, and SSAs could be developed for loading of poorly water-soluble CUR by controlling the sol-gel of silica precursor as well as MMA polymerization in the n-heptane/water interface. Impor-

tantly, changing the n-heptane/water volume ratio had a significant impact on particle size and, to a lesser extent, pore diameter. The results indicated that MSNs with large SSAs and wide pores could load CUR at high LA% and LE%, respectively. The loading parameters may be influenced by factors such as the CUR/MSN weight ratio, temperature, and incubation time. These findings highlight the importance of using MSNs to load and deliver CUR, which needs further research using XRD, DSC, TEM, and adsorption isotherm methods for a thorough understanding of CUR loading. In addition, a release study should be conducted depending on the final dosage form and route of administration for a specialized therapeutic application of CUR-loaded MSNs.

Acknowledgments

The authors gratefully acknowledge the use of the facilities of the Center for Nanotechnology in Drug Delivery at Shiraz University of Medical Sciences (SUMS). This study was financially supported by Shiraz University of Medical Sciences, Shiraz, Iran.

Conflict of Interest

None declared.

References

1. Yallapu MM, Nagesh PK, Jaggi M, Chauhan SC. Therapeutic Applications of Curcumin Nanoformulations. *AAPS J.* 2015 Nov;17(6):1341-56. doi: 10.1208/s12248-015-9811-z. Epub 2015 Sep 3. PMID: 26335307; PMCID: PMC4627456.
2. Karewicz A, Bielska D, Gzyl-Malcher B, Kepczynski M, Lach R, Nowakowska M. Interaction of curcumin with lipid monolayers and liposomal bilayers. *Colloids Surf B Biointerfaces*. 2011 Nov 1;88(1):231-9. doi: 10.1016/j.colsurfb.2011.06.037. Epub 2011 Jul 1. PMID: 21778041.
3. Abedanzadeh, M., et al., Curcumin loaded polymeric micelles of variable hydrophobic lengths by RAFT polymerization: Preparation and in-vitro characterization. *J Drug Deliv Sci Technol.* 2020. 58: p. 101793.
4. Gong C, Wu Q, Wang Y, Zhang D, Luo F, Zhao X, Wei Y, Qian Z. A biodegradable hydrogel system containing curcumin encapsulated in micelles for cutaneous wound healing. *Biomaterials.* 2013 Sep;34(27):6377-87. doi: 10.1016/j.biomaterials.2013.05.005. Epub 2013 May 29. PMID: 23726229.
5. Parvathy, K., P. Negi, and P. Srinivas, Curcumin–amino acid conjugates: synthesis, antioxidant and antimutagenic attributes. *Food Chem*. 2010. 120(2): 523-30.
6. Nandiyanto ABD, Kim S-G, Iskandar F, Okuyama K. Synthesis of spherical mesoporous silica nanoparticles with nanometer-size controllable pores and outer diameters. *Microporous Mesoporous Mater.* 2009;120(3):447-53.
7. Iskandar F, Lenggoro IW, Kim TO, Nakao N, Shimada M, Okuyama K. Fabrication and characterization of SiO2 particles generated by spray method for standards aerosol. *J Chem Eng Japan.* 2001;34(10):1285-92.
8. Kao K, Mou C. Pore-expanded mesoporous silica nanoparticles with alkanes/ethanol as pore expanding agent. *Microporous Mesoporous Mater.* 2013;169:7-15.
9. Kilpeläinen M, Riikonen J, Vlasova MA, Huotari A, Lehto VP, Salonen J, et al. In vivo delivery of a peptide, ghrelin antagonist, with mesoporous silicon microparticles. *J Control Release.* 2009 Jul 20;137(2):166-70. doi: 10.1016/j.jconrel.2009.03.017. Epub 2009 Apr 2. PMID: 19345247.
10. Chen JF, Ding HM, Wang JX, Shao L. Preparation and characterization of porous hollow silica nanoparticles for drug delivery application. *Biomaterials.* 2004 Feb;25(4):723-7. doi: 10.1016/s0142-9612(03)00566-0. PMID: 14607511.
11. Vasconcelos T, Sarmento B, Costa P. Solid dispersions as strategy to improve oral bioavailability of poor water soluble drugs. *Drug Discov Today.* 2007 Dec;12(23-24):1068-75. doi: 10.1016/j.drudis.2007.09.005. Epub 2007 Oct 30. PMID: 18061887.
12. Sachs-Barrable K, Lee SD, Wasan EK, Thornton SJ, Wasan KM. Enhancing drug absorption using lipids: a case study presenting the development and pharmacological evaluation of a novel lipid-based oral amphotericin B formulation for the treatment of systemic fungal infections. *Adv Drug Deliv Rev.* 2008 Mar 17;60(6):692-701. doi: 10.1016/j.addr.2007.08.042. Epub 2007 Nov 5. Erratum in: Adv Drug Deliv Rev. 2008 Dec

14;60(15):1675. PMID: 18053611.
13. Dinda AK, Prashant CK, Naqvi S, Unnithan J, Samim M, Maitra A. Curcumin loaded organically modified silica (ORMOSIL) nanoparticle; a novel agent for cancer therapy. *Int J Nanotechnol.* 2012;9(10):862.
14. Kim S, Stébé M,a Blina J, Pasc A. pH-controlled delivery of curcumin from a compartmentalized solid lipid nanoparticle@ mesostructured silica matrix. *J Mater Chem B*. 2014;2(45):7910-17.
15. Patra, D. and F. Sleem. A new method for pH triggered curcumin release by applying poly (l-lysine) mediated nanoparticle-congregation. *Anal. Chim Acta*. 2013;795:60-8.
16. Li N, Wang Z, Zhang Y, Zhang K, Xie J, Liu Y, et al. Curcumin-loaded redox-responsive mesoporous silica nanoparticles for targeted breast cancer therapy. *Artif Cells Nanomed Biotechnol.* 2018;46(sup2):921-935. doi: 10.1080/21691401.2018.1473412. Epub 2018 May 23. PMID: 29790797.
17. Lv Y, Li J, Chen H, Bai Y, Zhang L. Glycyrrhetinic acid-functionalized mesoporous silica nanoparticles as hepatocellular carcinoma-targeted drug carrier. *Int J Nanomedicine.* 2017 Jun 12;12:4361-4370. doi: 10.2147/IJN.S135626. PMID: 28652738; PMCID: PMC5476610.
18. Radhakrishnan K, Tripathy J, Datey,bc Chakravortty A.D, RaichurA.M. Mesoporous silica–chondroitin sulphate hybrid nanoparticles for targeted and bio-responsive drug delivery. *New J Chem*. 2015;39(3):1754-60.
19. Sun X, Wang N, Yang LY, Ouyang XK, Huang F. Folic Acid and PEI Modified Mesoporous Silica for Targeted Delivery of Curcumin. *Pharmaceutics.* 2019 Aug 23;11(9):430. doi: 10.3390/pharmaceutics11090430. Erratum in: Pharmaceutics. 2020 Jul 03;12(7): PMID: 31450762; PMCID: PMC6781278.
20. Xu X, Lü S, Gao C, Feng C, Wu C, Bai X, et al. Self-fluorescent and stimuli-responsive mesoporous silica nanoparticles using a double-role curcumin gatekeeper for drug delivery. *Chem Eng J.* 2016;300:185-92.
21. Zhang Y, Zhi Z, Jiang T, Zhang J, Wang Z, Wang S. Spherical mesoporous silica nanoparticles for loading and release of the poorly water-soluble drug telmisartan. *J Control Release.* 2010 Aug 3;145(3):257-63. doi: 10.1016/j.jconrel.2010.04.029. Epub 2010 May 5. PMID: 20450945.
22. Shafiee M, Abolmaali S, Abedanzadeh M, Abedi M, Tamaddon A. Synthesis of Pore-Size-Tunable Mesoporous Silica Nanoparticles by Simultaneous Sol-Gel and Radical Polymerization to Enhance Silibinin Dissolution. *Iran J Med Sci.* 2021 Nov;46(6):475-486. doi: 10.30476/ijms.2020.86173.1595. PMID: 34840388; PMCID: PMC8611219.
23. Shafiee M, Abolmaali SS, Tamaddon AM, Abedanzadeh M, Abedi M. One-pot synthesis of poly (alkyl methacrylate)-functionalized mesoporous silica hybrid nanocomposites for microencapsulation of poorly soluble phytochemicals. *Colloids Interface Sci Commun*. 2020;37:100298.
24. Sreelola V, Sailaja AK, Pharmacy M. Preparation and characterisation of ibuprofen loaded polymeric nanoparticles by solvent evaporation technique. *Int J Pharm Pharm Sci.* 2014;6(8):416-421.
25. Freidus LG, Kumar P, Marimuthu T, Pradeep P, Choonara YE. Theranostic Mesoporous Silica Nanoparticles Loaded With a Curcumin-Naphthoquinone Conjugate for Potential Cancer Intervention. *Front Mol Biosci.* 2021 May 20;8:670792. doi: 10.3389/fmolb.2021.670792. PMID: 34095225; PMCID: PMC8173119.
26. Taebnia N, Morshedi D, Yaghmaei S, Aliakbari F, Rahimi F, Arpanaei A. Curcumin-loaded amine-functionalized mesoporous silica nanoparticles inhibit α-synuclein fibrillation and reduce its cytotoxicity-associated effects. *Langmuir*. 2016;32(50):13394-402.
27. Basavarajappa S, Chandramohan G, Davim JP. Application of Taguchi techniques to study dry sliding wear behaviour of metal matrix composites. *Mater Des*. 2007;28(4):1393-8.
28. Wang Y, Shan Y, Chen KZ, Gao L. Mesoporous Silica Nanoparticles with Controllable Pore Size: Preparation and Drug Release. *AMR* 2013;774-776:536-9.
29. Abdous B, Sajjadi SM, Ma'mani L. β-Cyclodextrin modified mesoporous silica nanoparticles as a nano-carrier: Response surface methodology to investigate and optimize loading and release processes for curcumin delivery. *J Appl Biomed.* 2017;15(3):210-8.
30. Bolouki A, Rashidi L, Vasheghani-Farahani E, Piravi-Vanak Z. Study of mesoporous

silica nanoparticles as nanocarriers for sustained release of curcumin. *Int J Nanosci Nanotechnol.* 2015;11(3):139-46.
31. Daryasari MP, Akhgar MR, Mamashli F, Bigdeli B, Khoobi M. Chitosan-folate coated mesoporous silica nanoparticles as a smart and pH-sensitive system for curcumin delivery. *Rsc Advances*. 2016;6(107):105578-88.
32. Kuang G, Zhang Q, He S, Liu Y. Curcumin-loaded PEGylated mesoporous silica nanoparticles for effective photodynamic therapy. *RSC advances.* 2020;10(41):24624-30.
33. Ma'mani L, Nikzad S, Kheiri-Manjili H, Al-Musawi S, Saeedi M, Askarlou S, et al. Curcumin-loaded guanidine functionalized PEGylated I3ad mesoporous silica nanoparticles KIT-6: practical strategy for the breast cancer therapy. *Eur J Med Chem*. 2014 Aug 18;83:646-54. doi: 10.1016/j.ejmech.2014.06.069. Epub 2014 Jun 28. PMID: 25014638.
34. Elbialy NS, Aboushoushah SF, Sofi BF, Noorwali A. Multifunctional curcumin-loaded mesoporous silica nanoparticles for cancer chemoprevention and therapy. *Microporous Mesoporous Mater.* 2020;291:109540.
35. Ghosh S, Dutta S, Sarkar A, Kundu M, Sil PC. Targeted delivery of curcumin in breast cancer cells via hyaluronic acid modified mesoporous silica nanoparticle to enhance anticancer efficiency. *Colloids Surf B Biointerfaces*. 2021 Jan;197:111404. doi: 10.1016/j.colsurfb.2020.111404. Epub 2020 Oct 25. PMID: 33142257.
36. Kong ZL, Kuo HP, Johnson A, Wu LC, Chang KLB. Curcumin-Loaded Mesoporous Silica Nanoparticles Markedly Enhanced Cytotoxicity in Hepatocellular Carcinoma Cells. *Int J Mol Sci.* 2019 Jun 14;20(12):2918. doi: 10.3390/ijms20122918. PMID: 31207976; PMCID: PMC6628080.
37. Yadav YC, Pattnaik S, Swain K. Curcumin loaded mesoporous silica nanoparticles: assessment of bioavailability and cardioprotective effect. *Drug Dev Ind Pharm.* 2019 Dec;45(12):1889-1895. doi: 10.1080/03639045.2019.1672717. Epub 2019 Oct 7. PMID: 31549866.
38. Harini L, Srivastava S, Gnanakumar GP, Karthikeyan B, Ross C, Krishnakumar V, et al. An ingenious non-spherical mesoporous silica nanoparticle cargo with curcumin induces mitochondria-mediated apoptosis in breast cancer (MCF-7) cells. *Oncotarget.* 2019 Feb 5;10(11):1193-1208. doi: 10.18632/oncotarget.26623. PMID: 30838091; PMCID: PMC6383822.
39. Mohebian Z, Babazadeh M, Zarghami N. In Vitro Efficacy of Curcumin-Loaded Amine-Functionalized Mesoporous Silica Nanoparticles against MCF-7 Breast Cancer Cells. *Adv Pharm Bull.* 2022.
40. Mondal S, Ghosh S, Moulik SP. Stability of curcumin in different solvent and solution media: UV–visible and steady-state fluorescence spectral study. *J Photochem Photobiol B, Biol* 2016;158:212-8.
41. Abedi M, Abolmaali SS, Abedanzadeh M, Borandeh S, Samani SM, Tamaddon AM. Citric acid functionalized silane coupling versus post-grafting strategy for dual pH and saline responsive delivery of cisplatin by Fe3O4/carboxyl functionalized mesoporous SiO2 hybrid nanoparticles: A-synthesis, physicochemical and biological characterization. *Mater Sci Eng C*. 2019;104:109922.
42. Abedi M, Abolmaali SS, Abedanzadeh M, Farjadian F, Mohammadi Samani S, Tamaddon AM. Core-Shell Imidazoline-Functionalized Mesoporous Silica Superparamagnetic Hybrid Nanoparticles as a Potential Theranostic Agent for Controlled Delivery of Platinum(II) Compound. *Int J Nanomedicine.* 2020 Apr 20;15:2617-2631. doi: 10.2147/IJN.S245135. PMID: 32368044; PMCID: PMC7182466.
43. Soleimanpour M, Tamaddon AM, Kadivar M, Abolmaali SS, Shekarchizadeh H. Fabrication of nanostructured mesoporous starch encapsulating soy-derived phytoestrogen (genistein) by well-tuned solvent exchange method. *Int J Biol Macromol.* 2020 Sep 15;159:1031-1047. doi: 10.1016/j.ijbiomac.2020.05.124. Epub 2020 May 19. PMID: 32439450.
44. Mashayekhi S, Rasoulpoor S, Shabani S, Esmaeilizadeh N, Serati-Nouri H, Sheervalilou R, Pilehvar-Soltanahmadi Y. Curcumin-loaded mesoporous silica nanoparticles/nanofiber composites for supporting long-term proliferation and stemness preservation of adipose-derived stem cells. *Int J Pharm.* 2020 Sep 25;587:119656. doi: 10.1016/j.ijpharm.2020.119656. Epub 2020 Jul 18. PMID: 32687972.